ADVANCED MATERIALS

Supporting Information

for *Adv. Mater.*, DOI: 10.1002/adma.201101485

The Role of the Fabrication of Anatase-TiO_2 Chain-Networked Photoanodes

*Jing-Zhi Chen , Yin-Cheng Yen , Wen-Yin Ko , Ching-Yuan Cheng , and Kuan-Jiuh Lin **

Submitted to ADVANCED MATERIALS

Supporting Information

The Role of Fabrication of Anatase TiO_2 Chain-Networked Photoanodes

*Jing-Zhi Chen, Yin-Cheng Yen, Wen-Yin Ko, Ching-Yuan Cheng and Kuan-Jiuh Lin**

Department of Chemistry, National Chung Hsing University, Taichung 402, Taiwan

[*]Prof. K. J. Lin, J. Z. Chen, Y. C. Yen, Dr. W.Y Ko
Department of Chemistry,
National Chung Hsing University,
Taichung 402, Taiwan (ROC).
E-mail:kjlin@dragon.nchu.edu.tw

Dr. C. Y. Cheng
Experimental Facility Division
National Synchrotron Research Center
Hsinchu 30076, Taiwan (ROC).

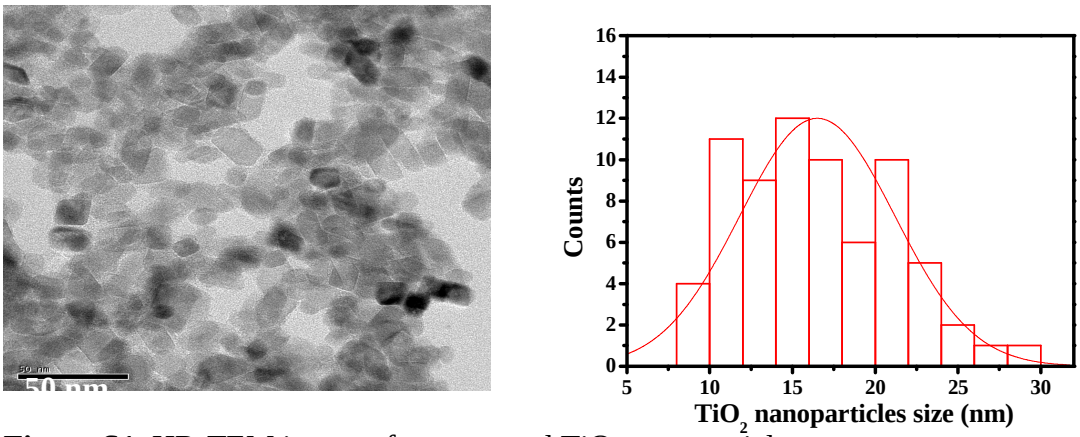

Figure S1. HR-TEM image of as-prepared TiO_2 nanoparticles.

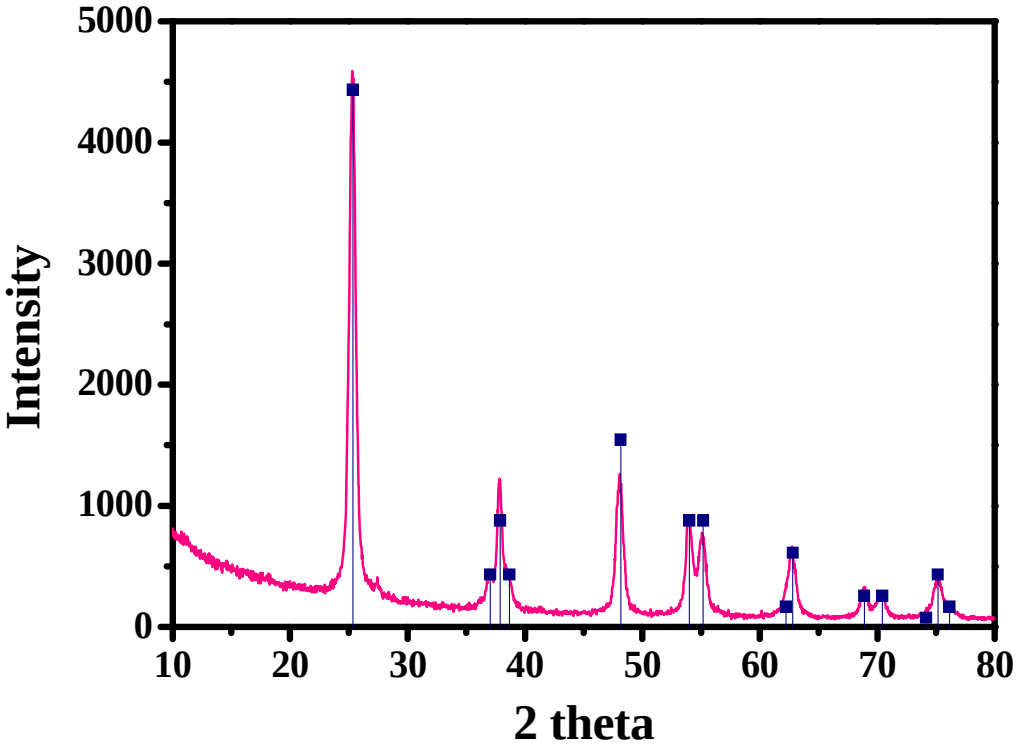

Figure S2. XRD pattern for as-prepared TiO_2 nanoparticles. The pattern shows that the corresponding diffraction peaks agree well with the diffraction line peaks for anatase in JCPDS 21-1272.

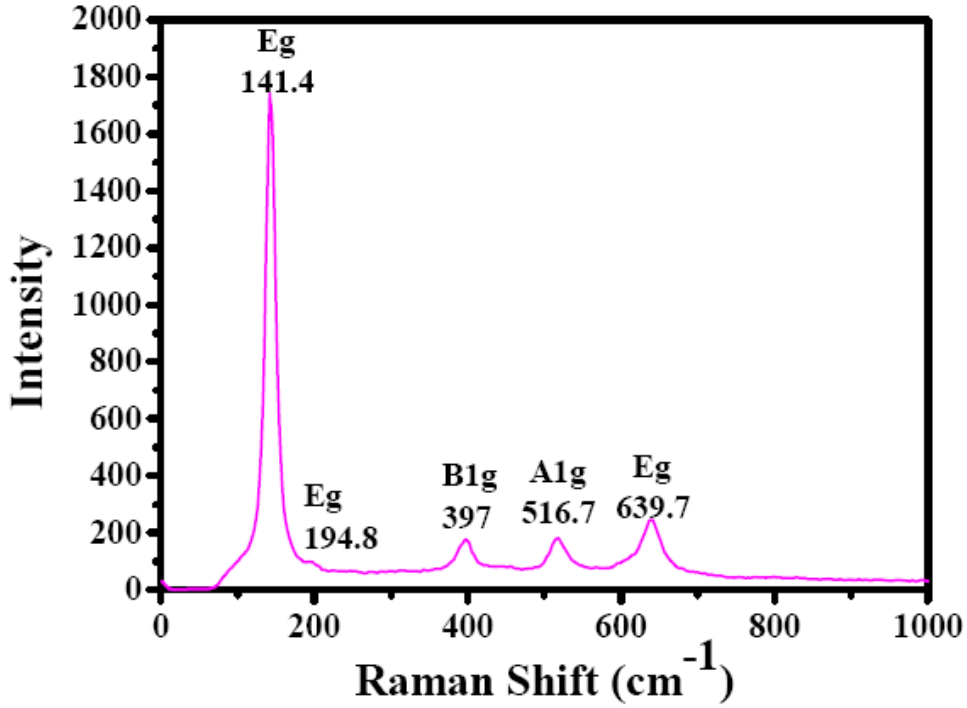

Figure S3. Raman spectrum for as-prepared TiO_2 nanoparticles.

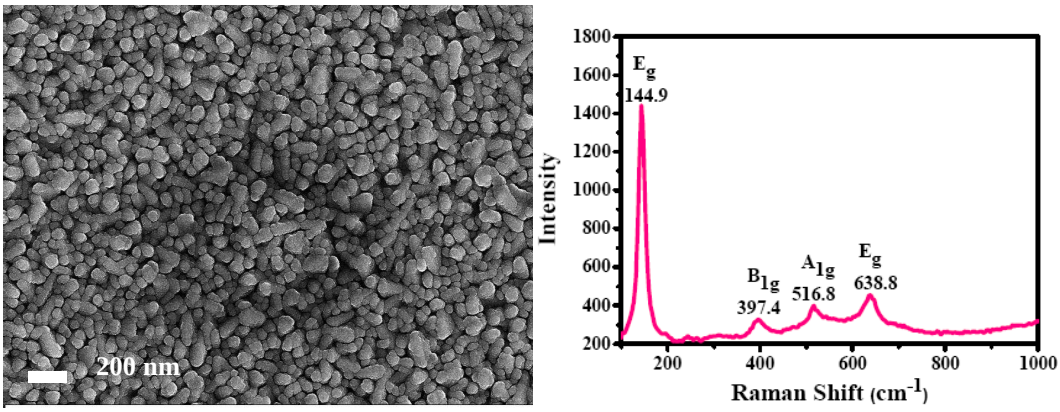

Figure S4. FE-SEM image (left) and Raman spectrum (right) for Ti (200nm)/FTO substrate calcined at 450 °C for 30 min, showing that the anatase TiO_2 film was formed and adhered to the FTO substrate.

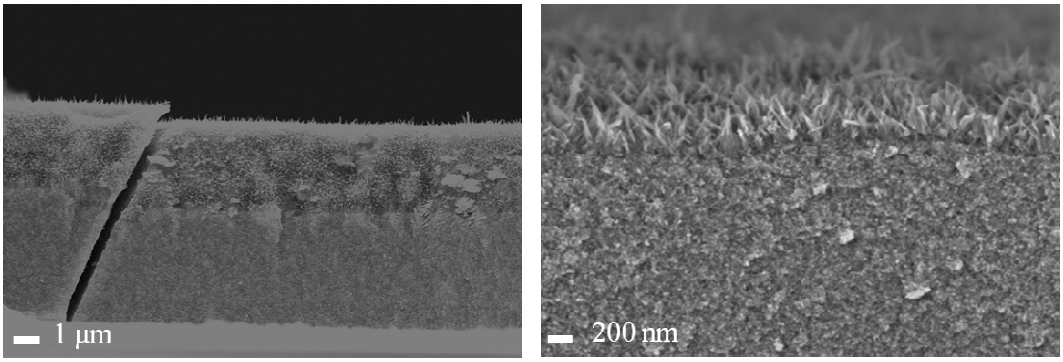

Figure S5. FESEM images of cross section of TiO_2 (7 μm)/Ti (200nm)/FTO substrate which was hydrothermally reacted in a 10 M NaOH aqueous solution in a Teflon-lined autoclave reactor (internal capacity of 25 mL), heated at 130 °C for 2 h, illustrating that a chain-like network partially formed on the top surface of the TiO_2 layer.

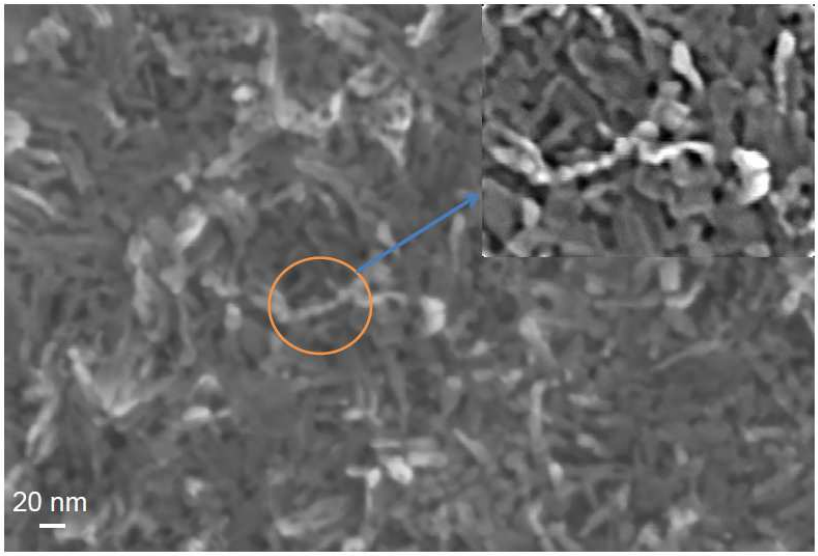

Figure S6. FESEM of chain network photoanode. The inset image shows one of the pearl-necklace chains

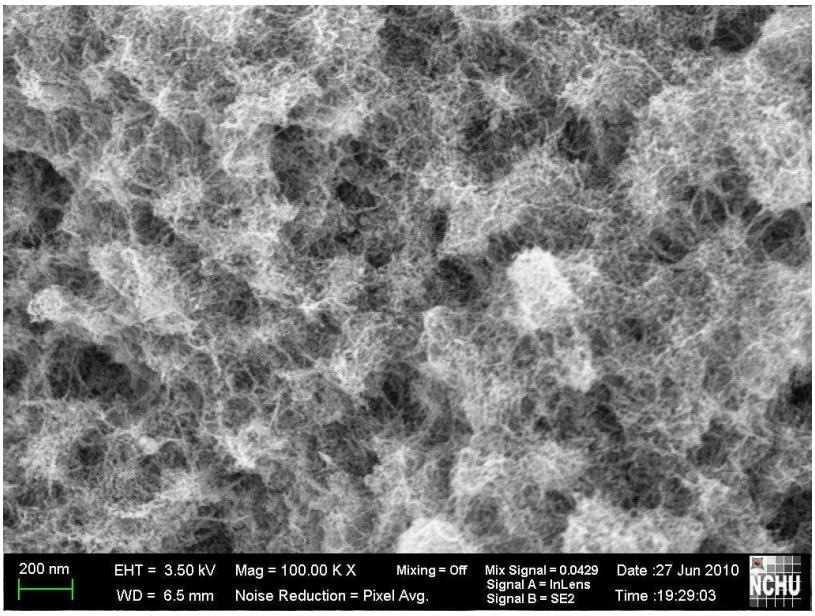

Figure S7. FE-SEM image of P25 (Degussa) nanoparticle-based photoanodes, The image shows that chain-like networks are obtained when the P-25 (Degussa) nanoparticles are employed as the TiO_2 layer in the sandwich-layered system. Notably, pear-necklace chains/fibers made of TiO_2 nanoparticles clearky formed under the same alkaline hydrothermal processing conditions.

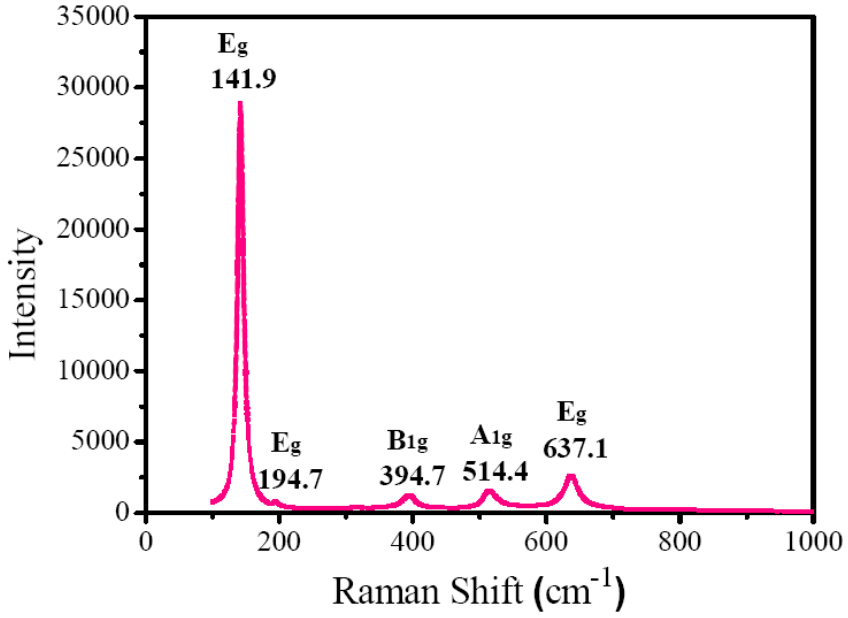

Figure S8. Raman spectrum for representative 12-μm-thick chain-networked photoanode.

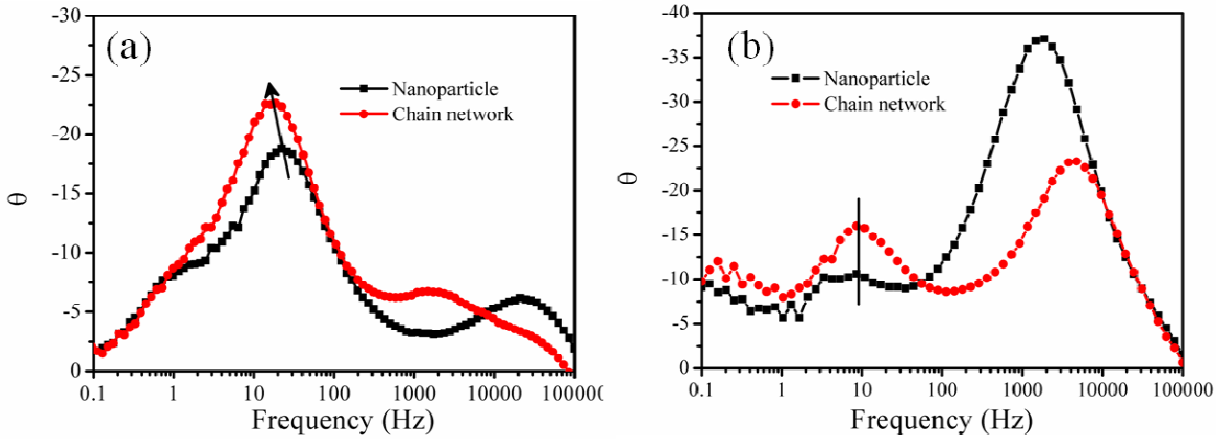

Figure S9. Bode phase plot of nanoparticle-based and chain-networked devices in a)liquid electrolyte and b)oligomer electrolyte. All devices were measured under the open-circuit voltage condition at 1 sun. In **Fig. 4b**, the characteristic peak frequency in the central arc of both devices is the same; however, it is lower than that of the liquid devices, and no shift is observed in the Bode phase plot (**Fig. S9b**). This indicate that relative to the liquid electrolyte, the charege recombination rate in both devices is surpressed in oligomer electrolyte.

Table S1. Photovoltaic parameters of the liquid electrolyte-based dye-sensitized solar cells. The active areas were about 0.196 cm^2.

Photoanodes	J_{sc} (mA cm^{-2})	V_{oc} (V)	*FF*	Efficiency (%)	Dye-loading (10^{-7} mol/L)
Chain network	15.48 ± 0.73	0.74 ± 0.01	0.68 ± 0.02	7.72 ± 0.43	31.1
Nanoparticles	16.28 ± 0.46	0.72 ± 0.02	0.71 ± 0.02	8.25 ± 0.26	58.9

Table S2. Photovoltaic parameters of the oligomer electrolyte-based dye-sensitized solar cells. The active areas were about 0.283 cm^2.

Photoanodes	J_{sc} (mA cm^{-2})	V_{oc} (V)	*FF*	Efficiency (%)
Nanoparticles (12 μm)	6.58 ± 0.62	0.58 ± 0.02	0.47 ± 0.06	1.83 ± 0.10
Chain network (7 μm)	9.05 ± 0.85	0.60 ± 0.02	0.40 ± 0.02	2.13 ± 0.17
Chain network (12 μm)	9.23 ± 0.35	0.61 ± 0.02	0.44 ± 0.04	2.49 ± 0.23